ARTICLE

BIOTECHNOLOGY and BIOENGINEERING

Dynamic Metabolic Flux Analysis Using a Convex Analysis Approach: Application to Hybridoma Cell Cultures in Perfusion

Sofia Fernandes de Sousa,[1] Georges Bastin,[2] Mario Jolicoeur,[3] Alain Vande Wouwer[4]

[1]Automatic Control Laboratory, University of Mons, 31 Boulevard Dolez, Mons 7000, Belgium; telephone: +32-065-374-128; fax: +32 65 37 41 36; e-mail: sofia.afonsofernandes@umons.ac.be

[2]Department of Mathematical Engineering, ICTEAM, Catholic University of Louvain, Louvain-La-Neuve, Belgium

[3]Department of Chemical Engineering, Laboratory in Applied Metabolic Engineering, Polytechnic University of Montreal, Montréal, Canada

[4]Automatic Control Laboratory, University of Mons, 7000 Mons, Belgium

ABSTRACT: In recent years, dynamic metabolic flux analysis (DMFA) has been developed in order to evaluate the dynamic evolution of the metabolic fluxes. Most of the proposed approaches are dedicated to exactly determined or overdetermined systems. When an underdetermined system is considered, the literature suggests the use of dynamic flux balance analysis (DFBA). However the main challenge of this approach is to determine an appropriate objective function, which remains valid over the whole culture. In this work, we propose an alternative dynamic metabolic flux analysis based on convex analysis, DMFCA, which allows the determination of bounded intervals for the fluxes using the available knowledge of the metabolic network and information provided by the time evolution of extracellular component concentrations. Smoothing splines and mass balance differential equations are used to estimate the time evolution of the uptake and excretion rates from this experimental data. The main advantage of the proposed procedure is that it does not require additional constraints or objective functions, and provides relatively narrow intervals for the intracellular metabolic fluxes. DMFCA is applied to experimental data from hybridoma HB58 cell perfusion cultures, in order to investigate the influence of the operating mode (batch and perfusion) on the metabolic flux distribution.

Biotechnol. Bioeng. 2015;9999: 1–11.

KEYWORDS: metabolic flux analysis; convex analysis; underdetermined system; mathematical modeling; hybridoma cells

Introduction

In the last decades, monoclonal antibodies (mAbs) have been increasingly used for medical research, diagnosis and therapy. The majority of the mAbs approved and under trials is produced by mammalian cells, such as chinese hamster ovary (CHO) and hybridoma cells, because of their capacity for proper protein folding, assembly and post-translational modification that result in full-active product (Chu and Robinson, 2001; Li et al., 2010; Reichert, 2012; Wurm, 2004). Knowledge of intracellular fluxes is of critical importance in the process of investigating and understanding cell metabolism. However, the experimental determination of metabolic fluxes in mammalian cells is a very complex task due to the high number of reactions and their highly bifurcated structure. All these problems introduce the need for a tool to determine the metabolic fluxes in the cell based on available and measurable data, giving rise to metabolic flux analysis (MFA) methods. Measurable data are usually obtained from extracellular measurements, such as, cell density, substrate and product concentrations.

Metabolic flux analysis (MFA) has been the subject of intense research for two decades. It is a useful tool to estimate in vivo metabolic fluxes in, among others, mammalian cell cultures. Determining in vivo fluxes provides quantitative information on the degree of engagement of various metabolic pathways in the overall cellular metabolism. The classical MFA method is used to study systems at metabolic steady state, meaning that intracellular fluxes do not change in time. This assumption is supported by the observation that intracellular dynamics are much faster than extracellular dynamics. Therefore, it makes sense to neglect the fast dynamics and consider that intracellular fluxes are in pseudo steady state (Stephanopoulos et al., 1998). This assumption is usually applied during the early exponential growth in batch cultures and in steady-state continuous cultures (Niklas and Heinzle, 2011).

When the environmental conditions of a culture change, dynamics should be considered to investigate cellular metabolism. To this end, the development of dynamic metabolic flux analysis (DMFA) techniques has been addressed (Leighty and Antoniewicz, 2011; Lequeux et al., 2010; Llaneras et al., 2012; Niklas et al., 2010; Vercammen et al., 2014). For instance, Lequeux et al. (2010) extended MFA based on the transformation of time series of

Correspondence to: S. Fernandes de Sousa
Contract grant sponsor: Interuniversity Attraction Poles Programme
Received 31 July 2015; Revision received 30 October 2015; Accepted 1 November 2015
Accepted manuscript online xx Month 2015;
Article first published online in Wiley Online Library (wileyonlinelibrary.com).
DOI 10.1002/bit.25879

concentration measurements into flux values. This transformation is based on differentiation of those time series. To avoid measurement noise amplification, a polynomial filtering was applied prior to the differentiation. This extended MFA technique was illustrated with *E. coli* cultures in which the limiting compound in the medium was changed from nitrogen to glucose and vice-versa. In the work of Niklas et al. (2010), dynamic changes in growth and metabolism of the new human cell line AGE1.HN were studied applying data smoothing on extracellular measurements using splines. Then, derivatives were calculated based on this smoothed data and dynamic intracellular fluxes were calculated using a classical MFA method. Leighty and Antoniewicz (2011) developed a new method for DMFA, where flux dynamics are described by piecewise linear flux functions. Since this method does not depend on taking derivatives, data smoothing and/or estimation of the average of the extracellular rates is not required. This method was illustrated with a fed-batch fermentation of *E. coli*, but is presented by the authors as a generic method (e.g., useful for microbial, mammalian and plant cells). In the work of Llaneras et al. (2012), dynamic extracellular concentration measurements are taken into account into a possibilistic MFA strategy by approximating the derivatives of the concentrations. This approach provides solution intervals, where the ranges of possible solutions are obtained by solving a set of minimum-maximum linear programming problems. Vercammen et al. (2014) presented a new methodology based on B-spline representation of the fluxes. These fluxes are estimated using dynamic optimization methods and tools, that is, orthogonal collocation, interior-point optimization and automatic differentiation. Furthermore, Akaike model discrimination criterion (AIC) (Burnham and Anderson, 2004) is used to estimate the free fluxes parameters and to determine the position of B-splines knots.

The advantage of DMFA compared to stationary MFA is that it provides information on metabolic transient, which cannot be observed using classical MFA. However, since DMFA is still based on stoichiometric metabolite balancing within an assumed metabolic model, DMFA carries the same limitations as MFA for resolving parallel pathways, cyclic pathways, and reversible reactions (Antoniewicz, 2015). Also, due to the complexity of the metabolic networks, measurable and available extracellular data is usually insufficient, leading to an underdetermined system of algebraic equations, whereby a unique solution cannot be computed. Therefore additional information is required to complement the extracellular flux data. Dynamic flux balance analysis (DFBA) was introduced by Mahadevan et al. (2002) to simulate the batch growth of *E. coli* on glucose. It was also further used to study the metabolism of mammalian cells (Gao et al., 2007; Nolan and Lee, 2011). The main challenge of DFBA is to determine an appropriate objective function (e.g., maximization of biomass production, ATP production, minimization of substrate utilization, etc.), which remains valid over the whole culture. Both DMFA and DFBA approaches combine metabolic network analysis based on pseudo steady-state assumption for intracellular metabolism with dynamic models for extracellular metabolites. The pseudo steady-state assumption in this situation is valid if the time-scale of the extracellular dynamics is longer than the time-scale for intracellular dynamics (Antoniewicz, 2013).

Isotopic tracer approaches for non-steady state flux analysis have also been introduced (Antoniewicz et al., 2007; Nöh et al., 2007; Young et al., 2008; Zamboni, 2011). However, this latter approach is cost and time expensive.

Besides DMFA, DFBA and isotopic tracer approaches, research has also developed towards detailed metabolic networks including information on the kinetics (Dorka et al., 2008; Ghorbaniaghdam et al., 2014), but those dynamic models require more experimental data for their validation. The identification of a priori unknown reaction kinetics is a critical task due to the model nonlinearity, relatively large number of parameters, and scarcity of informative experimental data.

In the present study, an alternative DMFA method is proposed, which is suitable for underdetermined systems, and does not require the definition of ad-hoc objective functions. The method is based on convex analysis, and builds upon the methodology introduced in (Provost and Bastin, 2004) and further exploited in (Zamorano et al., 2010). In these latter works, CHO batch cultures are considered and the cell life is divided into three phases: exponential growth, transition and death. In each of these phases, the specific uptake and production rates are assumed constant and are determined using linear regression. In this study, this assumption is waived, and mass balance differential equations for the extracellular concentrations, together with cubic spline smoothing, are used to assess the time evolution of the uptake and excretion rates. This information is then processed by convex analysis assuming that the intracellular species are in pseudo-steady state with respect to the time evolution of the extracellular concentrations (slow-fast approximation).

Dynamic Metabolic Flux Convex Analysis (DMFCA) allows determining bounded intervals for each intracellular flux, and makes the most of the available information (metabolic network and available extracellular measurements) without introducing additional constraints or objective function. In this work, DMFCA is applied to experimental data collected from hybridoma cultures operated in batch and perfusion modes, in order to get some insight into the changes in the metabolic fluxes between these two operating modes.

This paper is organized as follows. The next section provides information on the experimental databank, that is, data collected from cultures of hybridoma cell line HB58 in 2L bioreactor operated in batch and perfusion modes. The considered metabolic reaction network is also introduced, along with its main characteristics, including condition number, redundancy, and degrees of freedom. The DMFA problem is formulated, including extracellular dynamic mass balance equation, spline smoothing of the experimental data, and determination of bounded intervals for the intracellular fluxes using convex analysis. Then, the specific experimental application is discussed, with focus on the metabolic changes that can be observed between the initial batch phase and the subsequent perfusion phase.

Materials and Methods

Cell Line and Media

This study is illustrated with experimental data from hybridoma cell line HB58 (ATCC), which produces antibodies type IgG1, anti-CD54, specific for mouse kappa light chain. These experiments have been performed at the State Key Laboratory of Bioreactor Engineering,

East China University of Science and Technology (ECUST), Shanghai (Niu et al., 2013).

Serum-free medium chemically defined with 1:1 mixture of DMEM and F12 (Gibco) was used and supplemented with 10 mg of bovine insulin, 10 mg of transferring-selenite (Fe-saturated), 500 μmol of ethanolamine and other property additives. The culture medium was supplemented with 15 mM of glucose, 11.5 mM of glutamine and other amino acids (see Table SI of Supplementary Material).

Bioreactor Operation Mode

Perfusion cultures were conducted in a 2-L stirred bioreactor (B. Braun Biostat BDCU) and were settled in a working volume of 1.8 L. Culture started in batch mode and was inoculated to reach an initial concentration between $0.2–0.5 \times 10^9$ cells/L. Temperature was kept at 36.8°C; the gases air: CO_2, O_2, and N_2 were mixed to maintain DO at 40% air saturation and bicarbonate solution (0.75 mol/L Na_2CO_3 and 0.5 mol/L $NaHCO_3$) was used for pH control around 7.0 ± 0.2. Data acquisition and process control were performed using the supervisory software MFCS/Win 3.0. Perfusion phase started at 56.5 h with a constant dilution rate (D) of $0.0197\ h^{-1}$. Cells were retained by a spin-filter (20 μm) and the stirring speed was kept at 200 rpm.

Analysis Methods

Experimental data contain the time evolution of the extracellular concentrations of glucose, lactate, ammonia, eighteen amino acids (except proline and cysteine), biomass, and antibody (IgG1). Cells were counted with hemocytometer using the trypan blue exclusion method. The antibody concentration in the supernatant of HB58 culture was analyzed by a sandwich ELISA method with specific binding antibodies. The chemical formulas for biomass and antibody were determined to be $CH_{1.988}O_{0.4890}N_{0.2589}$ and $CH_{1.54}O_{0.3146}N_{0.2645}$, respectively.

Glucose, lactate and ammonia concentrations were determined using YSI 7100 biochemical analyzer (Yellow Springs Instruments). The eighteen amino acids were analyzed by reverse-phase High Performance Liquid Chromatography (HPLC) with a UV-visible detector.

Metabolic Network Model

The metabolic network considered in this work contains $r = 70$ biochemical reactions, $m = 44$ internal metabolites and $p = 22$ extracellular metabolites present in the culture medium, which are either substrates or products. It was constructed based on essentially two metabolic networks previously considered: the one of Provost (2006) containing 68 biochemical reactions and the one of Riveros (2012) involving 100 reactions. It embraces the major reactions of central metabolism such as glycolysis, Tricarboxylic Cycle Acid (TCA), amino acids metabolism and biomass and antibody synthesis (see Table I). In contrast with most bacteria and plants, which can synthesize the 20 common amino acids, mammals can only synthesize half of them. Mammalian cells cannot synthesize the so-called essential amino acids, which have to be provided in the culture medium. The nonessential amino acids are those that the cell is able to synthesize and the conditionally essential amino acids are those that the cell is able to synthesize under particular circumstances. Following this classification, only catabolic pathways are considered for essential amino acids, while both catabolic and anabolic pathways are taken into account for nonessential amino acids. Furthermore, biomass and antibody synthesis are also incorporated into the model and the stoichiometric coefficients are taken from (Niu et al., 2013). Biomass synthesis is described from its precursor building blocks by considering G6P (precursor required for the synthesis of lipids, ribose and deoxyribose in nucleotides) and amino acids (to proteins). Since R5P is not used in this work to describe cell growth rate, the pentose phosphate pathway is not included, thus simplifying the metabolic network. Concerning the nucleotide synthesis, the authors followed the same strategy as in (Gambhir et al., 2003) and then adapted in (Niu et al., 2013), where nucleotide synthesis is lumped into the biomass synthesis. It should be stressed that there is no exact metabolic network to represent cellular metabolism: a candidate metabolic network is based on available metabolic knowledge and built in a way that allows describing the consumption and production of extracellular metabolites in a satisfactory manner. However, special care has to be exercised to preserve the stoichiometry while lumping and/or combining reactions.

Note that convex analysis provides positive intervals (solutions); therefore the flux direction of the biochemical reactions is fixed a priori in agreement with the metabolic state of the cells.

Condition Number

The condition number C allows to determine whether the metabolic network is well or ill-conditioned as follows:

$$C(N_i^T) = \|N_i^T\|\|(N_i^T)^{\#}\| \tag{1}$$

where $\|\ \|$ indicates any matrix norm and $\left(N_i^T\right)^{\#}$ is the pseudo-inverse of the stoichiometric matrix $N_i^{44\times70}$ (see Equation 6). To evaluate Equation (1), singular value decomposition can be used. The largest singular values are found for both N_i^T and its pseudo-inverse $\left(N_i^T\right)^{\#}$ and the two values are multiplied (Stephanopoulos et al., 1998). A requirement for a well-conditioned stoichiometric matrix is that the condition number be between 1 and 100. If the condition number is greater than 100 the stoichiometric matrix is said ill-conditioned, and it may be necessary to modify the model. In our case, the condition number is 13.87; consequently, the representation of the metabolism is well-conditioned.

Extracellular Flux Determination

Extracellular fluxes of twenty-two metabolites can be determined based on the measurements of the time evolution of biomass, antibody, glucose, lactate, ammonia and eighteen amino acids, except proline, and cysteine.

Table I. Metabolic reactions for the metabolism of Hybridoma cells.

Flux	Metabolic reaction
Glycolysis	
v1	$Glc_{ext} + ATP \rightarrow G6P + ADP$
v2	$G6P \leftrightarrow F6P$
v3	$F6P + ATP \rightarrow DHAP + G3P + ADP$
v4	$DHAP \leftrightarrow G3P$
v5	$G3P + NAD^+ + ADP \leftrightarrow 3PG + NADH + ATP$
v6	$3PG + ADP \rightarrow Pyr + ATP$
Tricarboxylic acid cycle	
v7	$Pyr + NAD^+ + CoASH \rightarrow AcCoA + CO_2 + NADH$
v8	$AcCoA + Oxal + H_2O \rightarrow Cit + CoASH$
v9	$Cit + NAD(P)^+ \rightarrow \alpha KG + CO_2 + NAD(P)H$
v10	$\alpha KG + CoASH + NAD^+ \rightarrow SucCoA + CO_2 + NADH$
v11	$SucCoA + GDP + Pi \leftrightarrow Succ + GTP + CoASH$
v12	$Succ + FAD \leftrightarrow Fum + FADH_2$
v13	$Fum \leftrightarrow Mal$
v14	$Mal + NAD(P)^+ \leftrightarrow Oxal + NADH$
Pyruvate fates	
v15	$Pyr + NADH \leftrightarrow Lac_{ext} + NAD^+$
v16	$Pyr + Glu \leftrightarrow Ala + \alpha KG$
Anaplerotic reaction	
v17	$Mal + NAD(P)^+ \leftrightarrow Pyr + CO_2 + NAD(P)H$
Amino acids metabolism	
v18	$Glu + NAD(P)^+ \leftrightarrow \alpha KG + NH_4^+ + NAD(P)H$
v19	$Oxal + Glu \leftrightarrow Asp + \alpha KG$
v20	$Gln \rightarrow Glu + NH_4^+$
v21	$Thr + NAD^+ + CoASH \rightarrow Gly + NADH + AcCoA$
v22	$Ser + THF \leftrightarrow Gly + CH_2O + 5,10 - CH_2 - THF$
v23	$3PG + Glu + NAD^+ \rightarrow Ser + \alpha KG + NADH$
v24	$Gly + THF + NAD^+ \rightarrow CO_2 + NH_4^+ + 5,10 - CH_2 - THF + NADH$
v25	$Ser \rightarrow Pyr + NH_4^+$
v26	$Thr \rightarrow \alpha Kb + NH_4^+$
v27	$\alpha Kb + CoASH + NAD^+ \rightarrow PropCoA + NADH + CO_2$
v28	$PropCoA + HCO_3^- + ATP \rightarrow SucCoA + ADP + Pi$
v29	$Trp \rightarrow Ala + 2CO_2 + \alpha Ka$
v30	$Lys + 2\alpha KG + 3NAD(P) + FAD^+ \rightarrow \alpha Ka + 2Glu + 3NADPH + FADH_2$
v31	$\alpha Ka + CoASH + 2NAD^+ \rightarrow AcetoAcCoA + 2NADH + 2CO_2$
v32	$AcetoAcCoA + CoASH \rightarrow 2AcCoA$
v33	$Val + \alpha KG + CoASH + 3NAD^+ + FAD^+ \rightarrow PropCoA + Glu + CO_2 + 3NADH + FADH_2$
v34	$Ile + \alpha KG + 2CoASH + 2NAD^+ + FAD^+ \rightarrow AcCoA + Glu + CO_2 + 2NADH + FADH_2 + PropCoA$
v35	$Leu + \alpha KG + CoASH + NAD^+ + HCO_3^- + ATP + FAD^+ \rightarrow AcCoA + AcetoAc + Glu + CO_2 + NADH + ADP + FADH_2$
v36	$AcetoAc + SucCoA \rightarrow AcetoAcCoA + Succ$
v37	$Phe + NADH \rightarrow Tyr + NAD^+$
v38	$Tyr + \alpha KG \rightarrow Fum + AcetoAc + Glu + CO_2$
v39	$Met + Ser + THF + ATP \rightarrow Cys + \alpha Kb + NH_4^+ + CH_2O + 5,10 - CH_2 - THF + AMP$
v40	$Cys \rightarrow Pyr + NH_4^+$
v41	$Asn \leftrightarrow Asp + NH_4^+$
v42	$Arg \rightarrow Orn + urea$
v43	$Orn + \alpha KG \leftrightarrow Glu\gamma SA + Glu$
v44	$Glu\gamma SA + NAD(P)^+ \rightarrow Glu + NAD(P)H$
v45	$His + THF \rightarrow Glu + NH_4^+ + 5,10 - CH_2 - THF$
v46	$Orn + CarbP \rightarrow Cln$
v47	$C\,ln + Asp + ATP \rightarrow ArgSucc + AMP$
v48	$ArgSucc \rightarrow Arg + Fum$

(*Continued*)

TABLE I. (*Continued*)

Flux	Metabolic reaction
Biomass synthesis	
v49	0.0156Ala+0.0082Arg+0.0287Asp+0.0167G6P+0.0245Gln+0.0039Glu+ 0.0038His+0.0099Ile+0.0156Leu+0.0119Lys+0.0039Met+0.0065Phe+ 0.016Ser+0.0094Thr+0.004Tyr+0.0113Val → Biomass
Antibody synthesis	
v50	0.01101Ala+0.00503Arg+0.00723Asn+0.00818Asp+0.01045Gln+0.0107Glu+0.0145Gly+ 0.0035His+0.005Ile+0.0142Leu+0.0145Lys+0.00283Met+0.00723Phe+0.02676Ser+ 0.001604Thr+0.00849Tyr+0.0189Val→Antibody(IgG)
Transport reactions	
v51	$Asp_{ext} \rightarrow Asp$
v52	$Gly \rightarrow Gly_{ext}$
v53	$Ser_{ext} \rightarrow Ser$
v54	$Glu \rightarrow Glu_{ext}$
v55	$Tyr_{ext} \rightarrow Tyr$
v56	$Ala \rightarrow Ala_{ext}$
v57	$Arg_{ext} \rightarrow Arg$
v58	$Asn_{ext} \rightarrow Asn$
v59	$G\ ln_{ext} \rightarrow G\ ln$
v60	$His_{ext} \rightarrow His$
v61	$Ile_{ext} \rightarrow Ile$
v62	$Leu_{ext} \rightarrow Leu$
v63	$Lys_{ext} \rightarrow Lys$
v64	$Met_{ext} \rightarrow Met$
v65	$Phe_{ext} \rightarrow Phe$
v66	$Thr_{ext} \rightarrow Thr$
v67	$Trp_{exp} \rightarrow Trp$
v68	$Val_{ext} \rightarrow Val$
v69	$NH_4^+ \rightarrow NH_{4ext}^+$
V70	$CO_2 \rightarrow CO_{2ext}$

The computation of these extracellular fluxes is based on mass balance differential equations, involving cellular growth (μ), substrate uptake (v_s) and product secretion (v_p), as described by:

$$\frac{dX}{dt} = (\mu - D\alpha)X \tag{2}$$

$$\frac{dS}{dt} = -DS - \upsilon_s X + DS_{in} \tag{3}$$

$$\frac{dP}{dt} = -DP + \upsilon_p X + DP_{in} \tag{4}$$

where X, S, P, S_{in}, P_{in}, and α denote biomass, substrate, product, influent substrate and product and biomass retention factor (in perfusion mode), respectively. The retention factor is given by Equation (5), where X_s represents the measured cell concentration inside the spin filter.

$$\alpha = 1 - \frac{X_s}{X} \tag{5}$$

Note that during batch cultures the dilution rate D is obviously equal to zero, so that Equations (2), (3), and (4) are simplified.

To evaluate the time derivatives appearing on the left-hand side of Equations (2–4), the experimental data are first smoothed off using smoothing B-splines (one for the batch phase and another one for the perfusion phase) (see Fig. 1).

Dynamic Metabolic Flux Analysis: Intracellular Flux determination

The goal of DMFA is to compute a set of admissible flux distributions continuously over time $v(t)$, using a pseudo-steady state assumption (no accumulation of internal metabolites):

$$\begin{pmatrix} N_i^{44\times 70} & 0 \\ N_m^{22\times 70} & -v_m^{22\times 1}(t) \end{pmatrix} \times \begin{pmatrix} v(t)^{70\times 1} \\ 1 \end{pmatrix} = 0 \tag{6}$$

where N_i is the stoichiometric matrix deduced from the metabolic network, N_m is the matrix connecting the fluxes to the available measurements and v_m represents the specific uptake and excretion rates of the measured extracellular species.

The metabolic network considered in this study involves 70 metabolic fluxes and $m = 44$ internal metabolites. The system is not redundant ($\text{rank}(N_i) = m = 44$), and with the information provided by 22 extracellular measurements, it is underdetermined with a degree of freedom of 4.

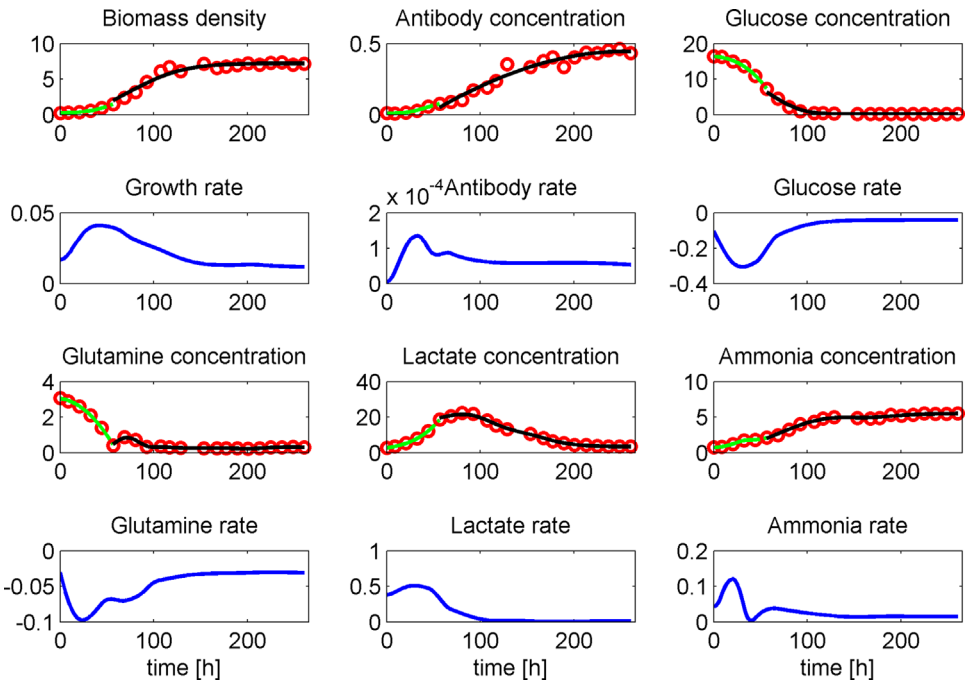

Figure 1. Extracellular flux determination using splines. Red dots: extracellular concentrations. Biomass density in [10^9 cells/L], antibody concentration in [g/L] and the others in [mM]. Green line: Spline over batch phase. Black line: Spline over perfusion phase. Blue line: Extracellular fluxes given in [mmol/10^9 cells.h]; except growth rate, which is in [h^{-1}].

The set of solutions to Equation (6) can be computed using convex analysis. This approach is based on the interpretation of elementary fluxes modes (simplest metabolic pathways linking substrates to products) and makes the most of the available information (i.e., metabolic network and extracellular measurements) without imposing any artificial constraint.

Geometrically speaking, the set of positive solutions of $N_i v(t) = 0$ generates a convex polyhedron cone S (see Fig. 2). Any flux distribution v in the cone S can be expressed as a non-negative linear combination of a set of elementary flux vectors e_i, which are the edges of the polyhedral cone S:

$$v(t) = w_1(t)e_1(t) + w_2(t)e_2(t) + \ldots + w_p(t)e_p(t), w_i(t) \geq 0 \quad (7)$$

If the system is further constrained with the information provided by the extracellular measurements (specific uptake and excretion rates), the solution space reduces to a convex polytope F in the positive orthant, where each admissible flux distribution $v(t)$ can be expressed as a convex combination of a set of non-negative basis vectors f_i which are the edges of this polytope. The set of admissible flux vectors is defined as:

$$v(t) = \sum_i w_i(t) f_i(t), \mathrm{w}_i(t) \geq 0, \sum_i w_i(t) = 1 \quad (8)$$

The basis vectors $f_i(t)$, the so-called elementary flux vectors of the flux space F, can be obtained with the software METATOOL (Pfeiffer et al., 1999), and in turn the admissible bounds $v_i^{\min}(t)$ and $v_i^{\max}(t)$for each admissible flux $v_i(t)$:

$$\begin{aligned} & v_j^{\min}(t) \leq v_j(t) \leq v_j^{\max}(t), \\ & \text{with} \\ & v_j^{\min}(t) = \operatorname{Min}_i f_i^j(t), v_j^{\max}(t) = \operatorname{Max}_i f_i^j(t) \end{aligned} \quad (9)$$

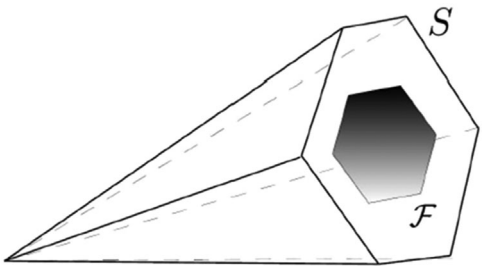

Figure 2. Convex polyhedron cones S and F (Riveros, 2012).

where $f_i^j(t)$ is the j-th component of the i-th basis vector $f_i(t)$.

The system is said well posed if the solution set is not empty and if all the metabolic fluxes are bounded. Otherwise, the system is said to be ill posed and additional extracellular information has to be provided.

Results

One of the objectives of this study is to evaluate and analyze the switch of hybridoma cell metabolism from batch to perfusion mode. Each of the 70 metabolic fluxes is now represented by bounded intervals determined using convex analysis continuously over time.

Firstly, a close inspection of the extracellular fluxes reveals the existence of a short lag phase at the beginning of the culture (first 8 h), which is excluded from the analysis.

Glycolysis Pathway

The rate of glycolysis is identical to the glucose uptake rate (see Fig. 3). The highest flux through the glycolytic pathway is observed in the exponential batch phase. Subsequently, it steadily decreases until 100 h, and remains nearly constant afterwards.

In several studies, the glycolytic activity is reported as the result of residual glucose concentration (Bonarius et al., 1996; Henry et al., 2005; Selvarasu et al., 2009).

Tricarboxylic Acid cycle

According to the DMFCA results, the major nutrient flux for the TCA cycle are glucose-derived pyruvate v6 (Fig. 3) and α-Ketoglutarate derived from glutamine metabolism v18 and v19 (Fig. 5). This observation corresponds to the phenomenon of glucose overflow metabolism (Amribt et al., 2013). The pyruvate generated from glycolysis is mostly metabolized via lactic acid fermentation and further reduced to lactate over the batch phase. However this is not verified in the transient from batch to perfusion phase, where pyruvate is mostly used to enter in the he TCA cycle to be oxidized to CO_2 (see Fig. 4). This means that cells switch to a more efficient metabolism using most of the pyruvate to obtain energy by means of the cellular respiration. In Sidorenko et al. (2008), a significant pyruvate dehydrogenase (PDH) complex activity was also found.

Pyruvate is also formed from TCA cycle intermediate malate represented by metabolic flux v17. Metabolic flux analysis indicates that the anaplerotic reaction catalyzed by malic enzyme (v17) and the amino acid serine (v25) are significant contributors to the production of pyruvate. In the work of Gambhir et al. (2003), malate shunt was also considered a significant contributor to the production of pyruvate. The fluxes centering on pyruvate are presented in Figure 4.

The anaplerotic reaction catalyzed by malic enzyme v17 is used to compensate the intermediates removed of the TCA cycle to serve as biosynthetic precursors (e.g., α-Ketoglutarate and oxaloacetate serve as precursors of amino acids aspartate and glutamate, respectively). As apparent from Figure 5, the metabolic flux v19 has the same behavior as the anaplerotic reaction. It can also be observed that the flux from succinate to malate (v12 and v13) is larger than the flux from oxaloacetate to citrate (v8) (see Fig. 6) due to the contribution of the anaplerotic reactions mainly in the form of α-Ketoglutarate. These results are in agreement with the ones obtained in the work of Paredes et al. (1998).

Amino Acid Metabolism

The lowest ratio between essential amino acid uptake rate and the corresponding stoichiometric coefficient for antibody synthesis gives an idea of which amino acid is the most used for antibody production. The (average) ratios are depicted in Figure 7, from which one can see that over the batch phase, valine is the most significant contributor to antibody production; while over the perfusion phase, valine, threonine, and lysine are the main contributors. The ratios of isoleucine and leucine are large, meaning that significant amounts of those were metabolized, probably for energy production. In Zamorano et al. (2010) the lowest ratio was found between threonine uptake rate and its stoichiometric coefficient for protein synthesis and the authors made the assumption that threonine was only used for protein production and not for catabolism purposes.

The conditionally or non-essential amino acids (aspartate, glycine, serine, glutamate, alanine, arginine, and asparagine) can be consumed or synthesized according to the cell needs. For instance, glycine is taken up over the batch phase (see Supplementary Material Fig. S2) and it is produced via glycine hydroxymethyltransferase

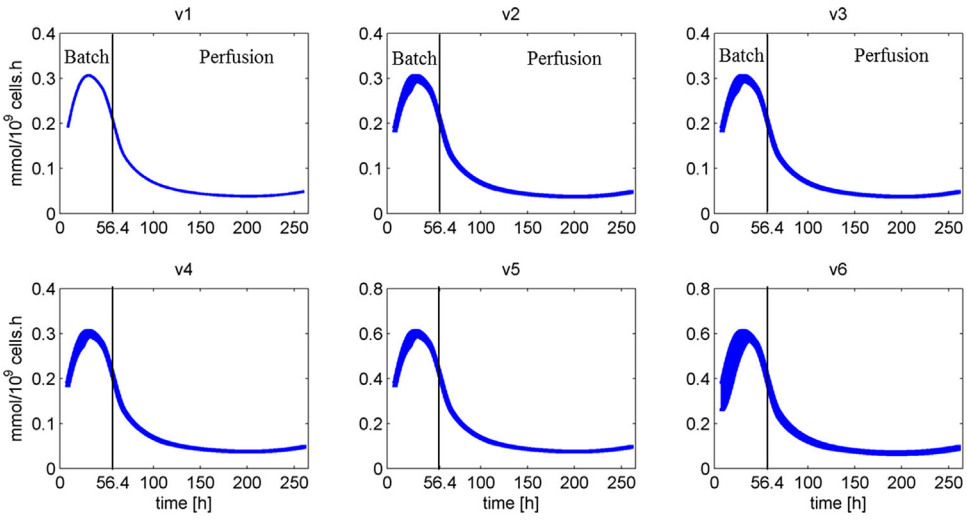

Figure 3. Dynamic evolution of glycolysis fluxes along culture time.

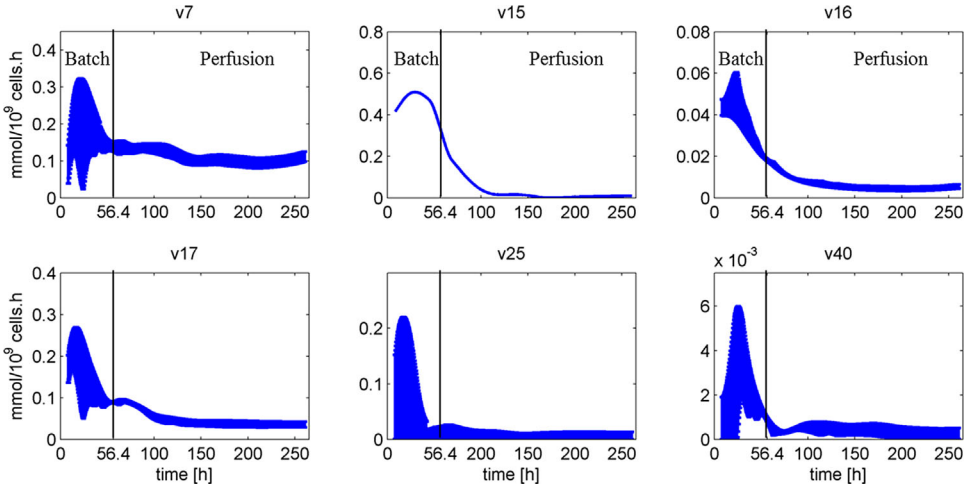

Figure 4. Dynamic evolution of pyruvate production and consumption fates along culture time.

indicated by Gly → Ser(v22). The opposite is observed over the perfusion phase, being then catalyzed by serine hydroxymethyltransferase. Sometimes, due to glucose depletion from the medium culture, the metabolism of the cells changes during this period and they can start consuming lactate and alanine instead of producing them in order to provide an alternative carbon and energy source for biosynthesis and growth. Glucose depletion is not a limitation and both alanine and lactate are produced over the whole culture. Given this fact, the direction of metabolic reactions v15 and v16 are defined as $Pyr+NADH \rightarrow Lac_{ext}+NAD^{+}$ and $Pyr+Glu \rightarrow Ala+\alpha KG$, respectively. Asparagine is produced over the batch phase and is produced over the perfusion phase through the asparagine synthase from aspartate (v41). Glutamate, arginine and aspartate are consumed over the whole culture (see Figs. S2 and S3 from Supplementary Material).

As observed in the work of Sanfeliu et al. (1997), when excessive amounts of glutamine are added to the hybridoma culture, glutamine is not efficiently used for cell growth, but rather to produce by-products, such as ammonia, alanine and proline. This fact is characterized as glutamine overflow metabolism (Amribt et al., 2013). Indeed looking at Figure 8 one can conclude that most of glutamine consumption is used to produce ammonia.

Respiratory Quotient (RQ)

The ratio between the carbon dioxide flux and oxygen flux is known as the respiratory quotient (RQ) (Equation 10). The range of RQ values reported for mammalian cells metabolism is around 1 (Frahm et al., 2002; Lovrecz and Gray, 1994; Niu et al., 2013), meaning that oxygen and carbon dioxide fluxes should be similar. The metabolic network considered allows the estimation of the carbon dioxide flux (v70). The values of oxygen uptake rate (OUR) were measured by modifying a dynamic method based on monitoring the decrease of

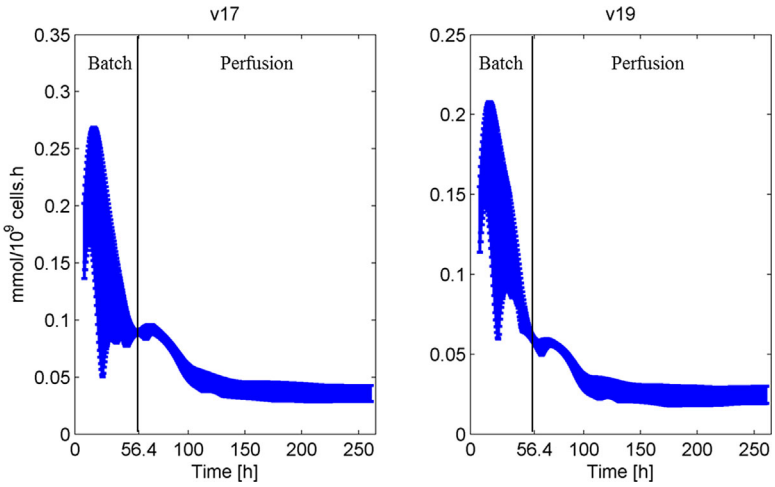

Figure 5. Dynamic evolution of anaplerotic reaction v17 as well as of precursors α-Ketoglutarate and oxaloacetate expressed in metabolic flux v19.

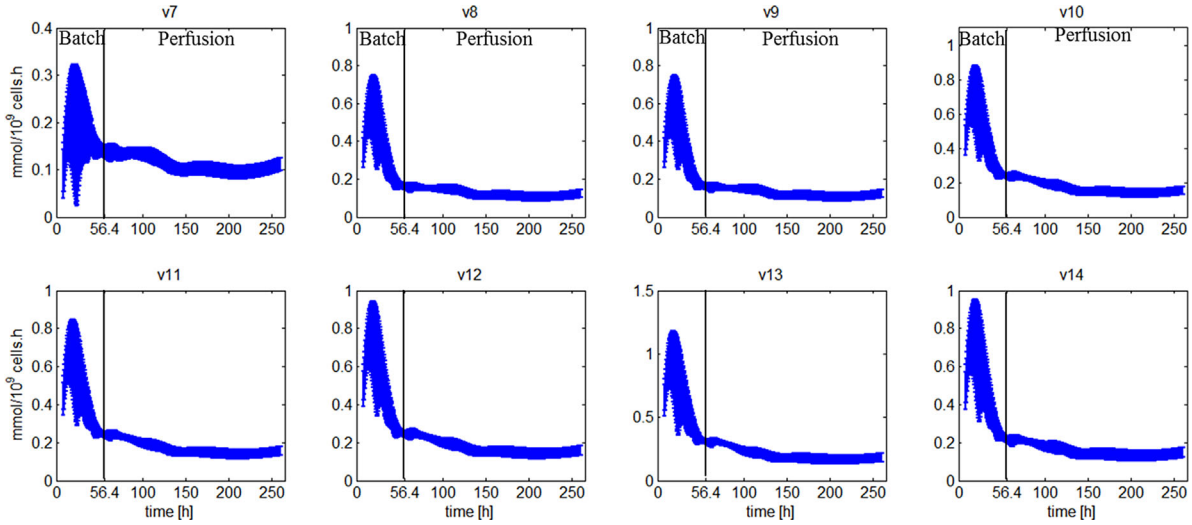

Figure 6. Dynamic evolution of TCA cycle fluxes along culture time.

the dissolved oxygen concentration over time. The detailed process is described in Niu et al. (2013). The oxygen flux can be obtained dividing OUR by the biomass concentration inside of the bioreactor X (Equation 11).

$$\mathrm{RQ} = \frac{v_{\mathrm{CO_2}}}{v_{\mathrm{O_2}}} \tag{10}$$

$$v_{\mathrm{O_2}} = \frac{\mathrm{OUR}}{X} \tag{11}$$

Both oxygen and carbon dioxide are depicted in Figure 9. There is a clear overestimation of the carbon dioxide flux, especially over the batch phase, where the respiratory quotient is outside of the range reported in literature. Despite the overestimation of RQ, the estimated carbon dioxide flux over the perfusion phase has the same order of magnitude as the one reported in Lovrecz and Gray (1994). In the work of Nolan and Lee (2011) an overestimation of RQ was also found, with a range of 1.5–2.8.

Conclusions

In this study, the metabolic flux analysis of hybridoma culture is achieved, using the classical pseudo steady-state assumption (no accumulation of internal metabolites) and under the constraints of the measurements of the time evolution of a number of culture components. Due to an insufficient number of measurements, the mass balance system is underdetermined.

In order to solve this underdetermined system and to quantify the metabolic fluxes continuously over time, a new approach is proposed: a dynamic metabolic flux analysis based on convex analysis (positive

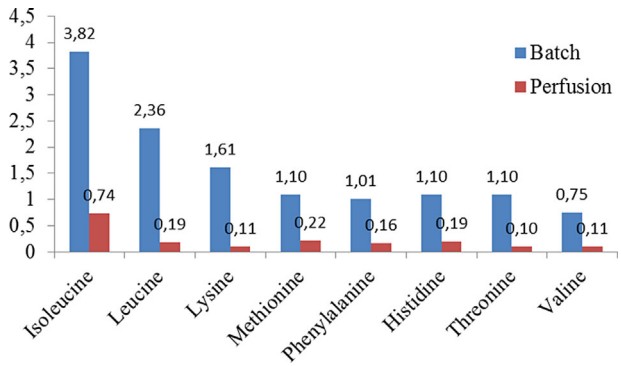

Figure 7. Ratio (in average) between essential amino acids uptake rate and its stoichiometry for cellular antibody. Blue: Batch phase. Red: Perfusion phase.

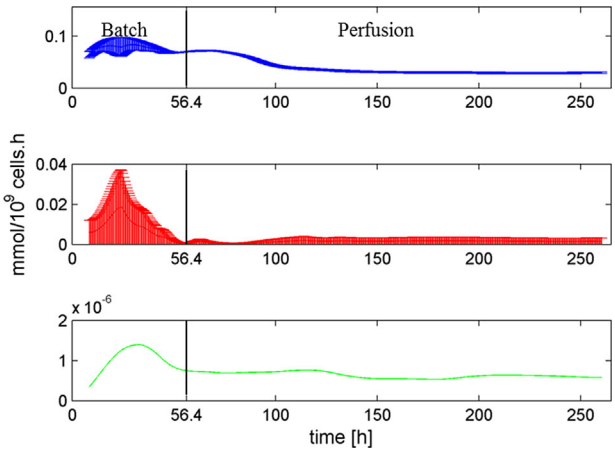

Figure 8. Dynamic evolution of glutamine consumption to produce ammonia given by flux v20 (blue), to produce biomass (defined as 0.0245 × v49) (red) and to participate in the antibody synthesis (defined as 0.01045 × v50) (green).

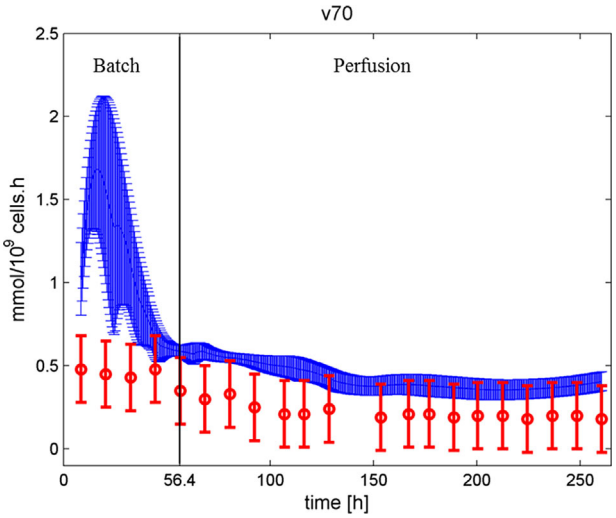

Figure 9. Blue intervals: Dynamic evolution of CO_2 flux determined by DMFA using convex analysis. Red dots: Oxygen uptake rate measurements considering a standard deviation of 10%, with an interval of confidence of 95%.

algebra). This method allows the determination of bounded intervals for the intracellular metabolic fluxes continuously over the culture time.

Classical MFA was extensively used in the past and it is a useful tool to analyze the cell average metabolism. However, from the results obtained applying DMFCA, one can see that the cells are not in steady state over the batch phase. Three phases are perfectly distinguishable: in the first 24 h cells are adapting to the culture medium; between 24 h and 36 h maximum growth rate is observable followed by growth rate decline mainly caused by the decrease in glucose and glutamine concentrations. When the perfusion mode starts, cells have to re-adapt to the new culture medium. As apparent from Figures 3–6, 8, and 9, steady-state metabolism is achieved around $t = 100$ h. The presented method, DMFCA, is well suited to describe the dynamic and adaptive behavior of the cells metabolism, allowing us to study the switch of the hybridoma metabolism from batch to perfusion.

During the batch phase, cell growth rate is exponential. Therefore, the uptake and production rates are larger than the ones in the steady state perfusion phase. One important advantage concerning the perfusion mode is the decrease of waste production (i.e., lactate and ammonia production rates are reduced), improving product quality. Consequently, one can conclude that cells switched to a more efficient metabolism using most of the pyruvate to obtain energy by means of the cellular respiration. Besides the switch from batch to perfusion, the relatively small amount of glucose feeding concentration also contributed to a more efficient metabolism. As discussed before, even if large amounts of glutamine were added to the culture, they were mostly used to produce ammonia (inhibitor) than to produce antibody or for cell growth.

This paper presents research results of the Belgian Network DYSCO (Dynamical Systems, Control, and Optimization), funded by the Inter-university Attraction Poles Programme initiated by the Belgian Science Policy Office. The authors are very grateful to Dr. Niu Hongxing for providing the experimental data and to Prof. Olivier Henry for insightful advice.

References

Amribt Z, Niu H, Bogaerts P. 2013. Macroscopic modelling of overflow metabolism and model based optimization of hybridoma cell fed-batch cultures. Biochem Eng J 70:196–209.

Antoniewicz MR. 2013. Dynamic metabolic flux analysis—Tools for probing transient states of metabolic networks. Curr Opin Biotechnol 24:973–978.

Antoniewicz MR. 2015. Methods and advances in metabolic flux analysis: A mini-review. J Ind Microbiol Biotechnol 42:317–325.

Antoniewicz MR, Kraynie DF, Laffend LA, González-Lergier J, Kelleher JK, Stephanopoulos G. 2007. Metabolic flux analysis in a nonstationary system: Fed-batch fermentation of a high yielding strain of *E. coli* producing 1,3-propanediol. Metab Eng 9:277–292.

Bonarius HPJ, Hatzimanikatis V, Meesters KPH, de Gooijer CD, Schmid G, Tramper J. 1996. Metabolic flux analysis of hybridoma cells in different culture media using mass balances. Biotechnol Bioeng 50:299–318.

Burnham KP, Anderson DR. 2004. Multimodel inference understanding AIC and BIC in model selection. Sociol Methods Res 33:261–304.

Chu L, Robinson DK. 2001. Industrial choices for protein production by large-scale cell culture. Curr Opin Biotechnol 12:180–187.

Dorka P, Fischer C, Budman H, Scharer JM. 2008. Metabolic flux-based modeling of mAb production during batch and fed-batch operations. Bioprocess Biosyst Eng 32:183–196.

Frahm B, Blank H-C, Cornand P, Oelßner W, Guth U, Lane P, Munack A, Johannsen K, Pörtner R. 2002. Determination of dissolved CO_2 concentration and CO_2 production rate of mammalian cell suspension culture based on off-gas measurement. J Biotechnol 99:133–148.

Gambhir A, Korke R, Lee J, Fu P-C, Europa A, Hu W-S. 2003. Analysis of cellular metabolism of hybridoma cells at distinct physiological states. J Biosci Bioeng 95:317–327.

Gao J, Gorenflo VM, Scharer JM, Budman HM. 2007. Dynamic metabolic modeling for a MAB bioprocess. Biotechnol Prog 23:168–181.

Ghorbaniaghdam A, Chen J, Henry O, Jolicoeur M. 2014. Analyzing clonal variation of monoclonal antibody-producing CHO cell lines using an in silico metabolomic platform. PLoS ONE 9. http://www.ncbi.nlm.nih.gov/pmc/articles/PMC3954614/

Henry O, Perrier M, Kamen A. 2005. Metabolic flux analysis of HEK-293 cells in perfusion cultures for the production of adenoviral vectors. Metab Eng 7:467–476.

Leighty RW, Antoniewicz MR. 2011. Dynamic metabolic flux analysis (DMFA): A framework for determining fluxes at metabolic non-steady state. Metab Eng 13:745–755.

Lequeux G, Beauprez J, Maertens J, Van Horen E, Soetaert W, Vandamme E, Vanrolleghem PA. 2010. Dynamic metabolic flux analysis demonstrated on cultures where the limiting substrate is changed from carbon to nitrogen and vice versa. BioMed Res Int 2010.

Li F, Vijayasankaran N, Shen (Yijuan) A, Kiss R, Amanullah A. 2010. Cell culture processes for monoclonal antibody production. mAbs 2:466–479.

Llaneras F, Sala A, Picó J. 2012. Dynamic estimations of metabolic fluxes with constraint-based models and possibility theory. J Process Control 22:1946–1955.

Lovrecz G, Gray P. 1994. Use of on-line gas analysis to monitor recombinant mammalian cell cultures. Cytotechnology 14:167–175.

Mahadevan R, Edwards JS, DoyleIII FJ. 2002. Dynamic flux balance analysis of diauxic growth in Escherichia coli. Biophys J 83:1331–1340.

Niklas J, Heinzle E. 2011. Metabolic flux analysis in systems biology of mammalian cells. In: Hu WS, Zeng A-P, editors. Genomics and Systems Biology of Mammalian Cell Culture. Heidelberg, Germany: Springer Berlin Heidelberg. p 109–132.

Niklas J, Schräder E, Sandig V, Noll T, Heinzle E. 2010. Quantitative characterization of metabolism and metabolic shifts during growth of the new human cell line AGE1.HN using time resolved metabolic flux analysis. Bioprocess Biosyst Eng 34:533–545.

Niu H, Amribt Z, Fickers P, Tan W, Bogaerts P. 2013. Metabolic pathway analysis and reduction for mammalian cell cultures—towards macroscopic modeling. Chem Eng Sci 102:461–473.

Nöh K, Grönke K, Luo B, Takors R, Oldiges M, Wiechert W. 2007. Metabolic flux analysis at ultra short time scale: Isotopically non-stationary 13C labeling experiments. J Biotechnol 129:249–267.

Nolan RP, Lee K. 2011. Dynamic model of CHO cell metabolism. Metab Eng 13:108–124.

Paredes C, Sanfeliu A, Cardenas F, Cairó JJ, Gòdia F. 1998. Estimation of the intracellular fluxes for a hybridoma cell line by material balances. Enzyme Microb Technol 23:187–198.
Pfeiffer T, Sánchez-Valdenebro I, Nuño JC, Montero F, Schuster S. 1999. METATOOL: For studying networks. Bioinformatics 15:251–257.
Provost A, Bastin G. 2004. Dynamic metabolic modelling under the balanced growth condition. J Process Control 14:717–728.
Provost A. 2006. Metabolic design of dynamic bioreaction models; Université catholique de Louvain. http://dial.academielouvain.be/vital/access/services/Download/boreal:5169/PDF_01
Reichert JM. 2012. Marketed therapeutic antibodies compendium. MAbs 4:413–415.
Riveros FZ. 2012. Metabolic Flux Analysis of CHO cell cultures; Université de Mons. http://perso.uclouvain.be/georges.bastin/thesezamorano.pdf
Sanfeliu A, Paredes C, Cairó JJ, Gòdia F. 1997. Identification of key patterns in the metabolism of hybridoma cells in culture. Enzyme Microb Technol 21:421–428.
Selvarasu S, Wong VVT, Karimi IA, Lee D-Y. 2009. Elucidation of metabolism in hybridoma cells grown in fed-batch culture by genome-scale modeling. Biotechnol Bioeng 102:1494–1504.
Sidorenko Y, Wahl A, Dauner M, Genzel Y, Reichl U. 2008. Comparison of metabolic flux distributions for MDCK cell growth in glutamine- and pyruvate-containing media. Biotechnol Prog 24:311–320.
Stephanopoulos G, Aristidou AA, Nielsen J. 1998. Metabolic engineering: Principles and methodologies. USA: Academic Press.
Vercammen D, Logist F, Impe JV. 2014. Dynamic estimation of specific fluxes in metabolic networks using non-linear dynamic optimization. BMC Syst Biol 8:132.
Wurm FM. 2004. Production of recombinant protein therapeutics in cultivated mammalian cells. Nat Biotech 22:1393–1398.
Young JD, Walther JL, Antoniewicz MR, Yoo H, Stephanopoulos G. 2008. An elementary metabolite unit (EMU) based method of isotopically nonstationary flux analysis. Biotechnol Bioeng 99:686–699.
Zamboni N. 2011. 13C metabolic flux analysis in complex systems. Curr Opin Biotechnol 22:103–108.
Zamorano F, Wouwer AV, Bastin G. 2010. A detailed metabolic flux analysis of an underdetermined network of CHO cells. J Biotechnol 150:497–508.

Supporting Information

Additional supporting information may be found in the online version of this article at the publisher's web-site.